

**Biophysical Journal**

**Supporting Material**

**Calcium Binding Promotes Conformational Flexibility of the Neuronal  
Ca<sup>2+</sup> Sensor Synaptotagmin**

Maria Bykhovskaia<sup>1,\*</sup>

<sup>1</sup>Neuroscience Department, Universidad Central del Caribe, Bayamon, Puerto Rico

## Supplemental Material

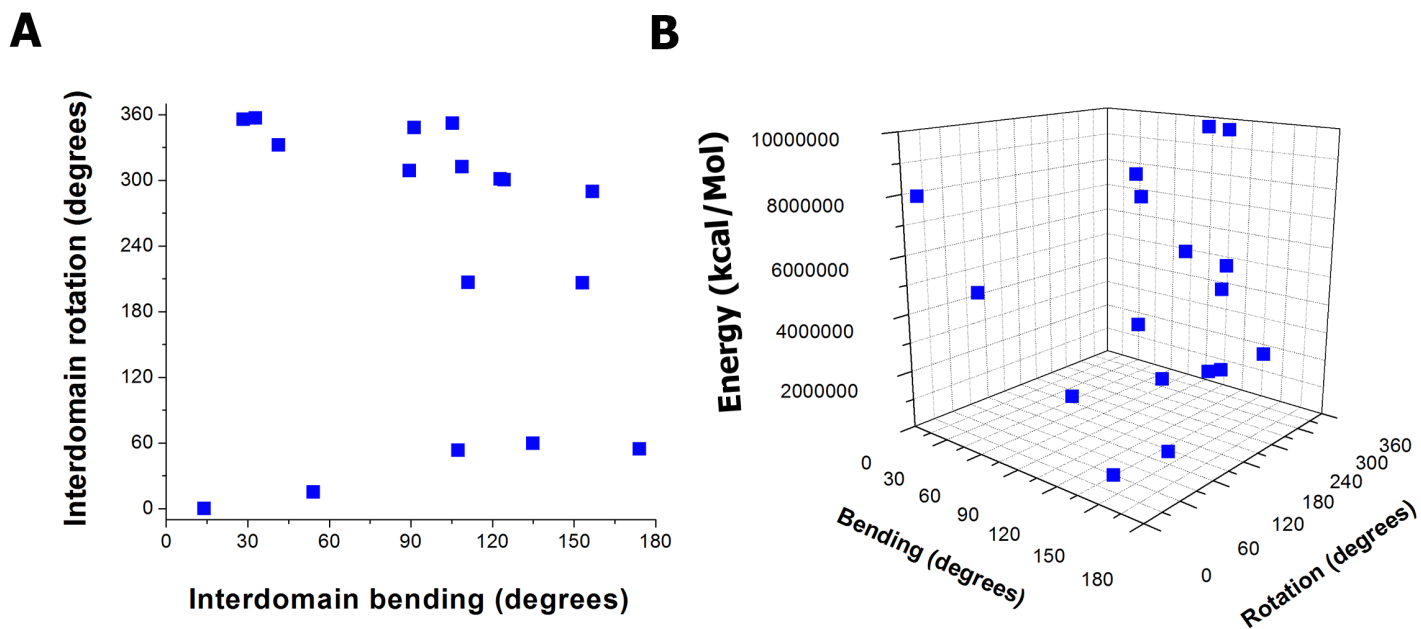


**Fig. S1.** MC sampling of Syt1 conformational space. The set of MC generated initial structures of Syt1 in the space of interdomain bending and rotation (A) and their energies (B) before optimization. The energy of the Syt1 conformation obtained by crystallography is taken as zero energy reference point.

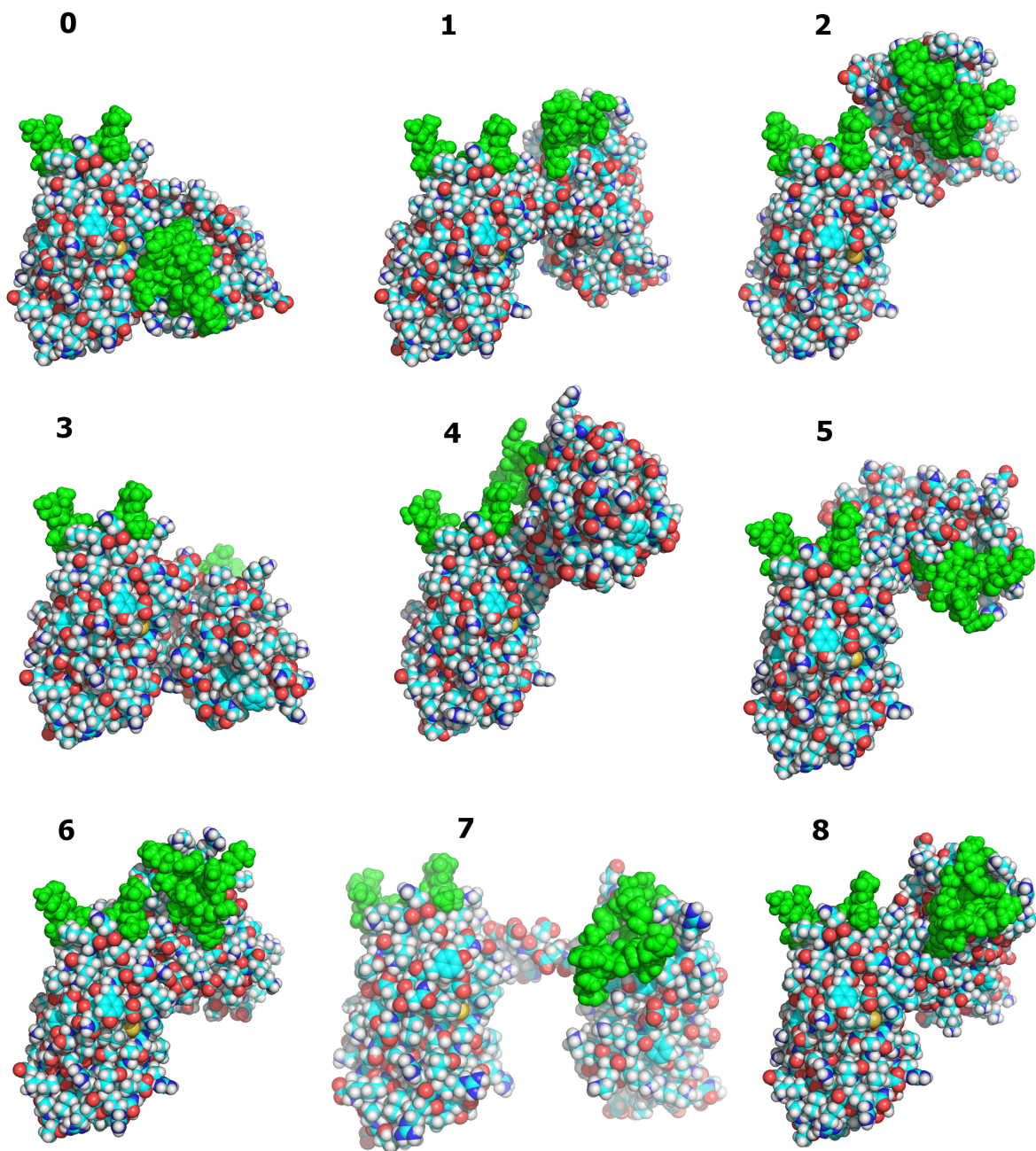


**Fig. S2.** Space filled models of the conformational states (1-8) generated employing MC smapling of the backbone tortsion angles of the linker and MCM-optimized. State 0 corresponds to the structure obained by crystallography. The structures are shown with a similar orientation of the C2B domain (left). Ca<sub>2</sub><sup>+</sup>-binding loops are colored green, the rest of the strucures are colored by the atom type: oxygen –red; carbon – cyan; hydrogen-while; nitrogen-blue.

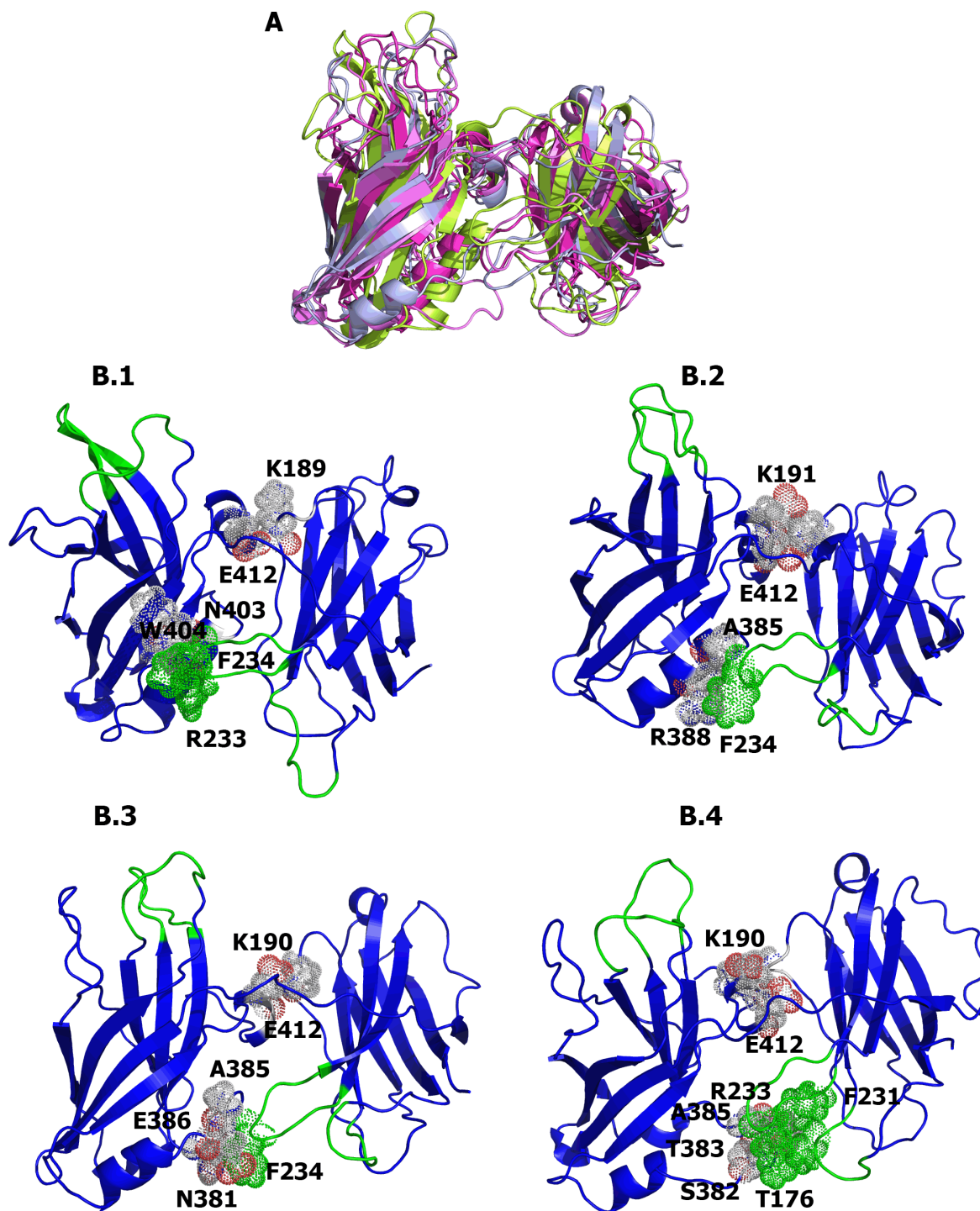


**Fig. S3.** Substates of the highly populated conformational state CS1. **A.** Four substates overlaid, showing mild variability in the backbone topology. **B.** Individual structures of four substates. Residues at the interface of C2 domains are shown as space filled models and labeled. All the residues of Ca<sup>2+</sup> binding loops are colored green.

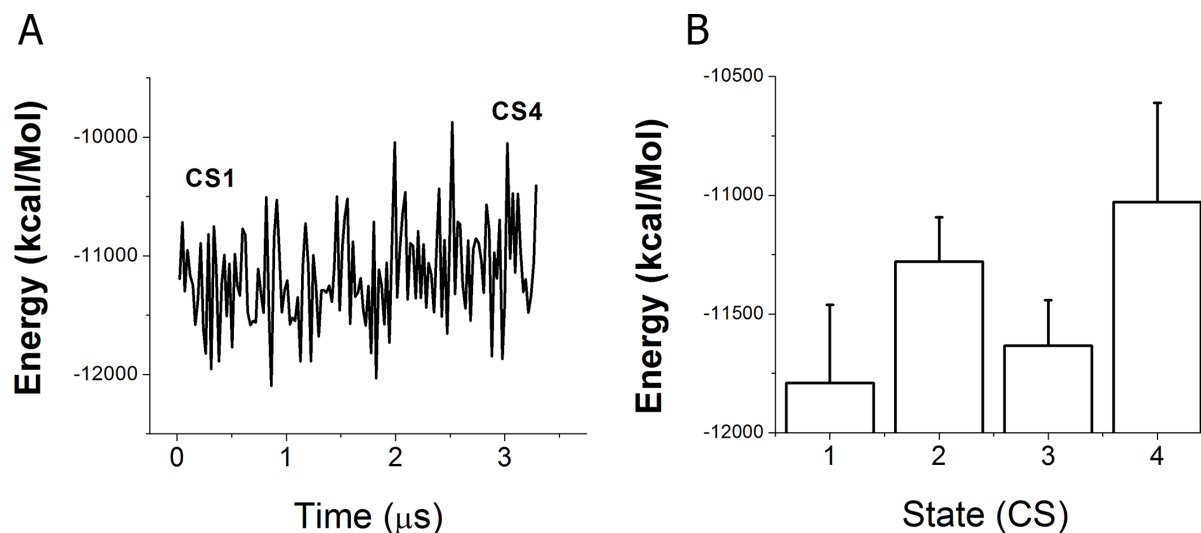


**Fig. S4.** Energies of Syt1 conformational states. The energy is computed as a sum of the energy of a protein and the energy of protein interactions with ions and water molecules. **A.** The energy along R0 trajectory (Table 1), representing a transition from the state CS1 to the state SC4. The energy was computed with a step of 100 points of the trajectory (2.4 ns). **B.** Average energies of Syt1 conformational states SC1-SC4. The bar graph shows mean  $\pm$  SD. Each data point was obtained as the average of 100 points (taken with a step of 2.4 ns) in the end of the trajectory which produced this state (R0s for SC1; R1 for SC2; R3 for SC3; R1 for SC4; see Table 1).

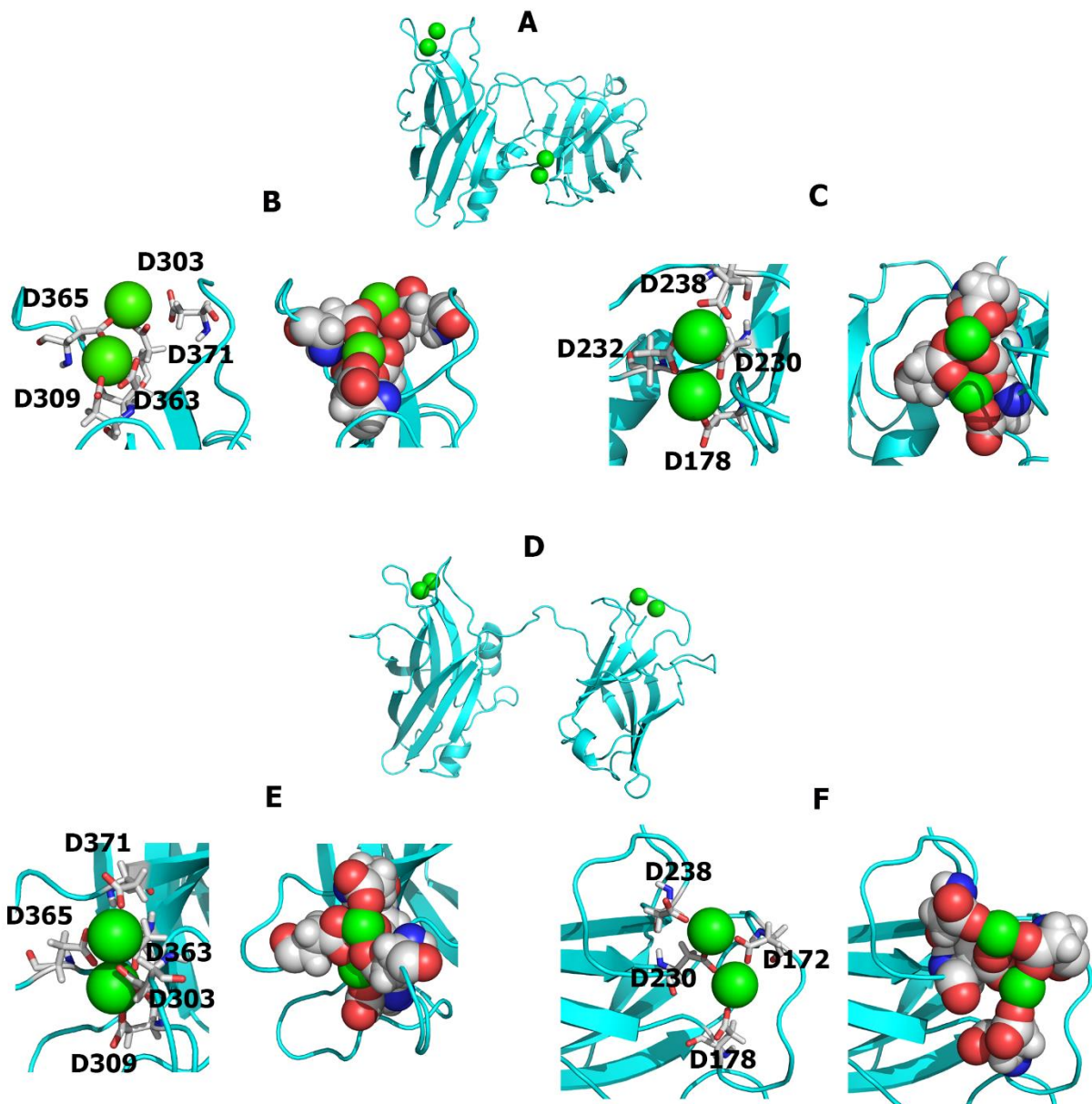


**Fig. S5.** Alternative  $\text{Ca}^{2+}$  bound forms of Syt1 obtained by MD simulations at elevated  $\text{Ca}^{2+}$  levels.  $\text{Ca}^{2+}$  ions are shown as green spheres. **A-C.**  $\text{Ca}^{2+}$  binding along the trajectory started from the state C1 (**A**). At C2B domain (**B**) two  $\text{Ca}^{2+}$  ions are chelated by aspartates D363, D365, D371, D309, and transient coordination bonds are formed with D303. At C2A domain, two  $\text{Ca}^{2+}$  ions are chelated by aspartates D178, D230, D232, and D283. **D-F.**  $\text{Ca}^{2+}$  binding along the trajectory started from a transient state with separated domains (**D**). At C2B domain (**E**) two  $\text{Ca}^{2+}$  ions are chelated by aspartates D363, D365, D371, D303, D309. At C2A domain, two  $\text{Ca}^{2+}$  ions are chelated by aspartates D172, D178, D230, and D238. In panels B, C, E, F, space filled models of  $\text{Ca}^{2+}$  ions surrounded by chelating aspartic acids are shown on the right.

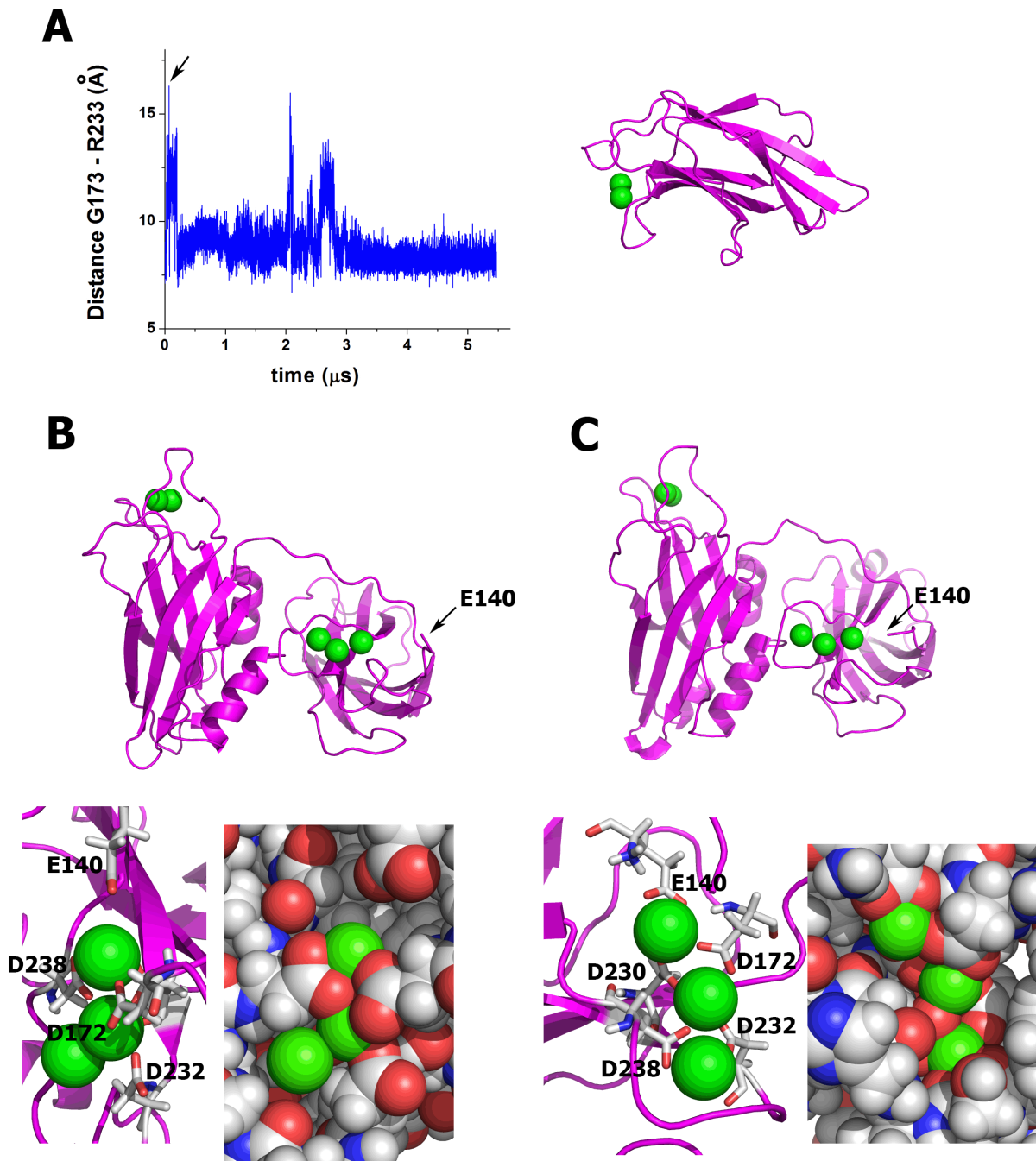


**Fig. S6.** Introducing three  $\text{Ca}^{2+}$  ions into C2A  $\text{Ca}^{2+}$  binding pocket. **A.** The distance between Ca atoms of the residues G173 and R233 along the trajectory R4Ca (Table 1) reflecting the distance between  $\text{Ca}^{2+}$  binding loops of C2A domain. Several transient increases in the distance indicate expansions of the  $\text{Ca}^{2+}$  binding pocket. The structure with the maximally opened pocket (arrow, C2A domain shown on the right) was selected to create the model of Syt1 form bound to five  $\text{Ca}^{2+}$  ions. **B.** The initial structure of the  $\text{Ca}^{2+}$ -bound Syt form. Two  $\text{Ca}^{2+}$  ions at the C2A domain are chelated by the residues D172, D232, D238, and D230 (the latter residue is shielded by  $\text{Ca}^{2+}$  ions), and the third ion occupies free space within the pocket. **C.** In the end of 250 ns simulation, two  $\text{Ca}^{2+}$  ions are chelated by the aspartates D172, D230, D232, and D238, while the third ion forms coordination bonds with the residue E140. N-terminus of Syt1 C2A-C2B fragment has moved to form contacts with C2A  $\text{Ca}^{2+}$  binding pocket.

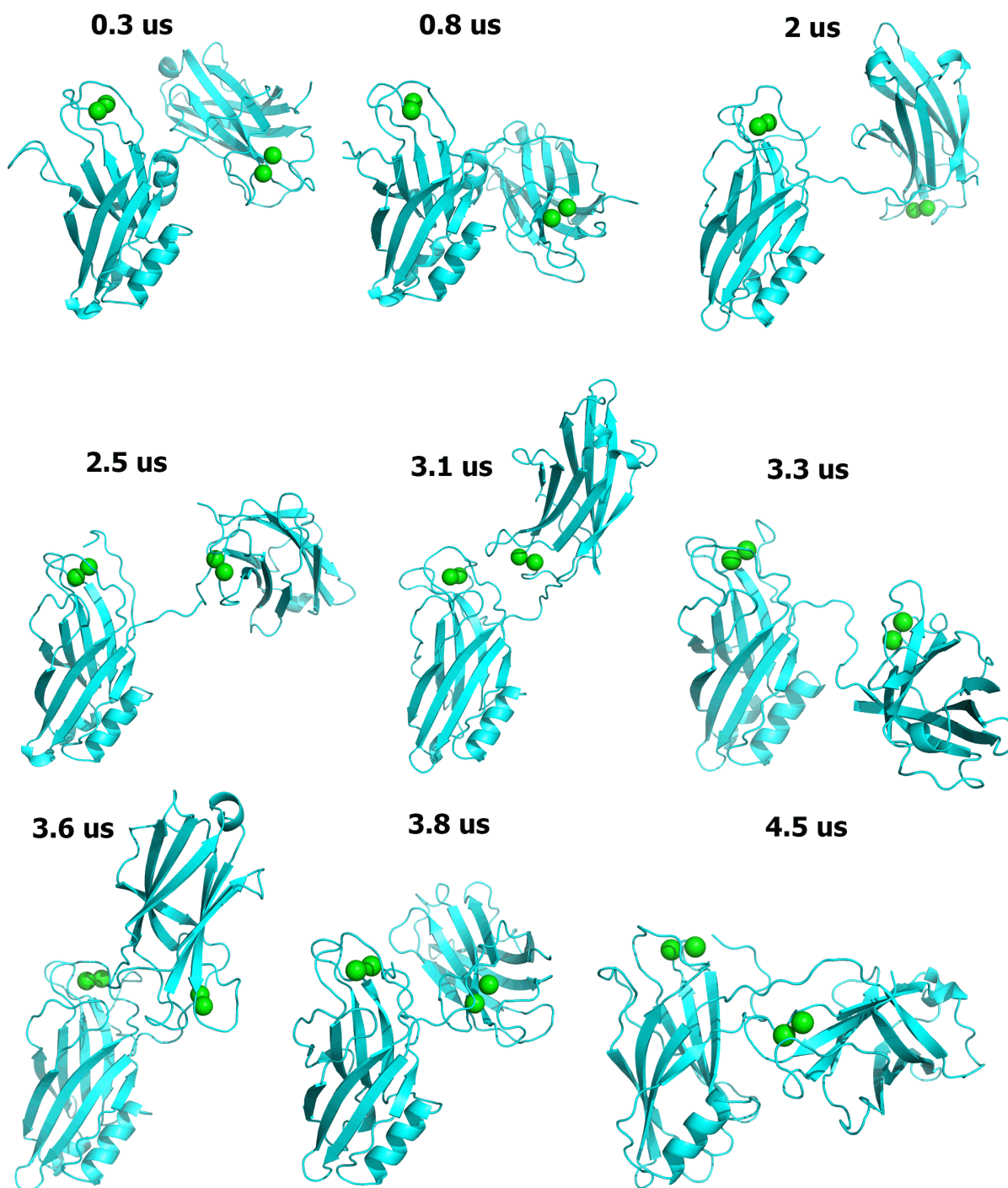


**Fig. S7.** Conformations of the  $\text{Ca}^{2+}$  bound Syt1 form along the 5.5  $\mu\text{s}$  MD trajectory (R4Ca, Table 1).  $\text{Ca}^{2+}$  ions are shown as green spheres, all the structures are shown with similar orientations of the C2B domain (left).



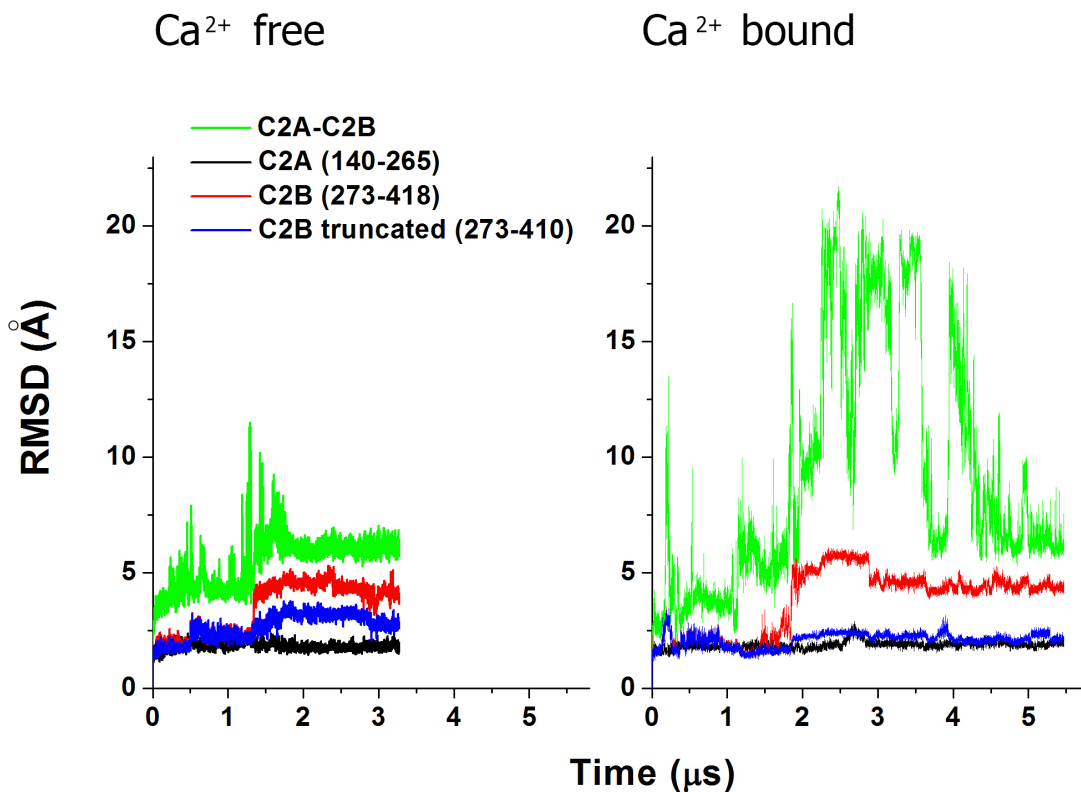


**Fig. S8.** The internal flexibility of C2 domains versus overall flexibility of C2A-C2B Syt1. RMSD was computed for backbone atoms only. RMSD for the Ca<sup>2+</sup> free form of Syt was computed along the R0 trajectory (Table 1). C2A and truncated C2B domains show low flexibility, also C-terminus C2B domains is flexible in both forms (compare C2B –red, versus truncated C2B –blue). The interdomain rearrangements increase flexibility (green line), and this flexibility is significantly stronger for the Ca<sup>2+</sup> - bound form.